Transgenerational metabolic disorders and reproduction defects induced by benzo[a]pyrene in Xenopus tropicalis

Marie Usal, Sylvie Veyrenc, Marie Darracq–Ghitalla-Ciock, Christophe Regnault, Sophie Sroda, Jean-Baptiste Fini, Cécile Canlet, Marie Tremblay-Franco, Muriel Raveton, Stephane Reynaud

Transgenerational metabolic disorders and reproduction defects induced by benzo[a]pyrene in *Xenopus tropicalis*

Marie Usal[1], Sylvie Veyrenc[1], Marie Darracq--Ghitalla-Ciock[1], Christophe Regnault[1], Sophie Sroda[1], Jean-Baptiste Fini[2], Cécile Canlet[3,4], Marie Tremblay-Franco[3,4], Muriel Raveton[1] and Stéphane Reynaud[1*].

[1] Univ. Grenoble-Alpes, Univ. Savoie Mont Blanc, CNRS, LECA, 38000 Grenoble, France.

[2] Unité PhyMA laboratory, Adaptation du Vivant, Muséum national d'Histoire naturelle, 7 rue Cuvier, 75005, Paris, France.

[3] Toxalim-Research Centre in Food Toxicology, Toulouse University, INRAE UMR 1331, ENVT, INP-Purpan, Paul Sabatier University, F-31027 Toulouse, France.

[4] Metatoul-AXIOM platform, National Infrastructure for Metabolomics and Fluxomics, MetaboHUB, Toxalim, INRAE UMR 1331, F-31027 Toulouse, France

*Corresponding Author:
Correspondence and requests for materials should be addressed to SR (stephane.reynaud@univ-grenoble-alpes.fr)

Email addresses: MU: marie.usal@hotmail.fr, SV: sylvie.veyrenc@univ-grenoble-alpes.fr, MDGC, marieghitalla@gmail.com, CR: christophe.regnault@gmail.com, SS: sophie.sroda@univ-grenoble-alpes.fr, JBF: fini@mnhn.fr, CC: cecile.canlet@inrae.fr, MTF: marie.tremblay-franco@inrae.fr, MR: muriel.raveton@univ-grenoble-alpes.fr, SR: stephane.reynaud@univ-grenoble-alpes.fr

Abstract

Metabolic disorders induced by endocrine disruptors (ED) may contribute to amphibian population declines but no transgenerational studies have evaluated this hypothesis. Here we show that *Xenopus tropicalis*, exposed from the tadpole stage, to the ED benzo[a]pyrene (BaP, 50 ng.L^{-1}) produced F2 progeny with delayed metamorphosis and sexual maturity. At the adult stage, F2-BaP females displayed fatty liver with inflammation, tissue disorganization and metabolomic and transcriptomic signatures typical of nonalcoholic steato-hepatitis (NASH). This phenotype, similar to that observed in F0 and F1 females, was accompanied by a pancreatic insulin secretory defect. Metabolic disrupted F2-BaP females laid eggs with metabolite contents significantly different from the control and these eggs did not produce viable progeny. This study demonstrated that an ED can induce transgenerational disruption of metabolism and population collapse in amphibians under laboratory conditions. These results show that ED benzo[a]pyrene can impact metabolism over multiple generations and support epidemiological studies implicating environmental EDs in metabolic diseases in humans.

Capsule abstract

Benzo[a]pyrene can induce transgenerational disruption of metabolism and population collapse in amphibians under laboratory conditions.

Keywords: endocrine disruptor, transgenerational, metabolic syndrome, amphibian population decline, *Xenopus tropicalis*

1. Introduction

Amphibians are one of the most impacted vertebrate group based on population declines with least at 41% of all known amphibian species are threatened with extinction (IUCN, 2019). Reasons for this decline include habitat loss, introduction of exotic species and emerging infectious diseases. Pollution of wetland habitats by endocrine disruptors (ED) may also be involved (Carey et al., 1999; Hayes et al., 2010a; Kiesecker, 2002). An endocrine disruptor is an exogenous substance or mixture that alters the function(s) of the endocrine system and consequently causes adverse health effects in an intact organism, or its progeny, or in (sub) populations (WHO, 2012). Field studies have suggested that ED may contribute to population decline in amphibians by altering population fitness (Fedorenkova et al., 2012) and amphibians might act as environmental sentinels (Hayes et al., 2010a). ED can interfere with the crosstalk between the thyroid and the reproductive axes in amphibians (Duarte-Guterman et al., 2014). ED can also disrupt organogenesis and gonadal differentiation in larvae (Crump et al., 2002; Hammond et al., 2015; Hayes et al., 2010b; Helbing, 2012; Langlois et al., 2010; Opitz et al., 2005) and egg and sperm maturation in adults (Hayes et al., 2011; Hayes et al., 2006; Hayes et al., 2002; Hayes et al., 2010b; Orton and Tyler, 2015; Safholm et al., 2014; Urbatzka et al., 2007). In addition their involvement in lasting alterations of immunity and resistance to infectious pathogens has been also highlighted (Robert et al., 2018; Robert et al., 2019). Studies on humans and other mammals suggest that metabolic disorders might be associated with ED (Casals-Casas and Desvergne, 2011; Chevalier and Fenichel, 2015, 2016). However, the involvement of ED exposure in the metabolic disorders associated with amphibian population decline has received little study. Initial evidence that ED can alter frog metabolism was documented in *Xenopus tropicalis* after acute exposure to triclosan and benzo[a]pyrene (BaP) (Regnault et al., 2016; Regnault et al., 2014). Controlled exposures of *X. tropicalis* throughout their life cycle to these two ED, alone or in mixtures at environmentally relevant concentrations, induced a metabolic syndrome featuring a pre-diabetic state. The treated frogs produced progeny with slower development, smaller adult size, and reduced reproductive success. These results link metabolic disorders to putative

87 population declines and highlight the potential multigenerational impacts of ED (Regnault et
88 al., 2018; Usal et al., 2019).

89 Studies in mammals and fishes show that ED may cause multi- and transgenerational effects
90 leading to reprotoxicity, cancer, metabolic impairments, obesity, diabetes, and
91 neurodegeneration in progeny that were not directly exposed (Chen et al., 2019a; Coimbra et
92 al., 2015; DeCourten et al., 2019; Perera et al., 2020; Skinner, 2014; Xie et al., 2019). The
93 transmission of ED effects across generations may result from epigenetic mechanisms
94 (Baker et al., 2014; Major et al., 2020; Perera et al., 2020). However, in many species, it is
95 believed that healthy offspring are born by a healthy mother (Swain and Nayak, 2009) since
96 offspring sustainability is dependent on female investment in the egg yolk (Hedayatirad et al.,
97 2020). Therefore, detrimental maternal effects on offspring could be explained by a lower
98 investment in egg reserves (Hedayatirad et al., 2020). Metabolic impairment of amphibian
99 females exposed to ED could affect progeny during several generations and the
100 transgenerational effects of ED could be a component of amphibian population declines.
101 We investigated the transgenerational impact of BaP on *Xenopus* females following F0
102 generation exposure from the tadpole to the mature adult stage at a concentration (50 $ng.L^{-1}$)
103 considered to be a safe level for drinking water (Health Canada, 2016; WHO, 2003).. BaP
104 was chosen because it is a widespread contaminant, classified as ED (USPEA; Petersen et
105 al., 2007) and it can markedly affect amphibian metabolism at the concentration used in this
106 study (Regnault et al., 2018). In addition, Ah-R ligands like BaP have been shown to induce
107 transgenerational effects in fish (Baker et al., 2014). In contrast to mammals, amphibian eggs
108 are fertilized in water and embryos develop externally. During BaP exposure of the parental
109 F0 generation, the F1 progeny are exposed only at the gamete stage. The gametes
110 producing the F2 frog generation are not exposed so the effects seen in F2 amphibians are
111 transgenerational (Baker et al., 2014). Although the purpose of this study was to investigate
112 the transgenerational impacts of BaP on the F2, putative metabolic disorders were observed
113 in F1 and F2 females to determine the phenotype transmission from F0 to F2 progeny. Here

we showed that this widespread ED can induce severe multi-and transgenerational metabolic disorders in female *Xenopus* leading to a total reproductive disruption at the F2. These data suggest that ED acting as metabolic disruptors may have a direct causal relationship with amphibian population decline and provide proof of their transgenerational effects in this phenomenon.

2. Material and methods

2.1. Ethics statement

All experiments were performed in an accredited animal house (LECA, n° C3842110001) and approved by the ethics committee ComEth Grenoble - C2EA – 12 (animal welfare agreement n° 02545.03).

2.2. Animals

F0 animals were exposed to 50 $ng.L^{-1}$ BaP from the seven-day old tadpole stage to mature adult stage as previously described (Regnault et al., 2018). This concentration matched BaP concentrations often found in polluted waters (Olivares-Rubio et al., 2015; Trapido and Ingeborg, 1996), and is below the maximum acceptable safe drinking water concentration (Health Canada, 2016; WHO, 2003). At the adult stage, five F0 females and ten F0 males were selected from the BaP treatment and from the control treatment and allowed to mate. The methods used are described in the SI.

2.3. Glucose tolerance test

Frogs were fasted 24 hours before the test. Glycaemia was measured by digital sampling at 0 and 8 hours after intraperitoneal glucose injection (1 $mg.g^{-1}$ fresh mass) using a glucometer (Accu-Chek Performa, Roche Diagnostics, Meylan, France).

2.4. Insulin resistance test

Frogs were fasted 12 hours before the test. Glycaemia was measured by digital sampling at 0 and 5 hours after injection of bovine insulin (Sigma Aldrich, France) in dorsal lymph sacs (5 $mU.g^{-1}$ fresh mass) using a glucometer (Accu-Chek Performa, Roche Diagnostics, Meylan, France).

147 *2.5. Histological observations*

148 The liver (same lobe/frog), the pancreas and the muscle were collected, embedded in Tissue
149 OCT (Labonord - VWR, Templemars, France), frozen in liquid nitrogen, and stored at -80°C.
150 Using a cryostat (CM3050 S, Leica, Nussloch, Germany), histological transverse sections 7
151 µm thick were produced and mounted on Super-Frost plus microscope slides (Labonord).
152 Staining procedures are described in the SI.

153

154 *2.6. Plasma insulin concentration measurements*

155 Insulinemia was measured in 24 hours-fasting F2 females or after a glucose challenge. The
156 methods used are described in the SI.

157

158 *2.7. Statistics*

159 For F1 and F2 females, phenotypic data are expressed as the mean ± SEM derived from 6 to
160 16 individual experiments, depending on the measured parameter (see Fig. legends). Since
161 the statistical distribution of the data was Gaussian for several data and not for other, a
162 Wilcoxon's test was used to compare the BaP-exposure population to the control population.
163 To statistically compare the percentage of F2 females showing pancreatic inflammation from
164 F2 control and F2-BaP populations a Khi² test was used.
165 The distributions of animal development times (age to metamorphosis) and female maturity
166 time for the F2 generation were compared between the control populations and the BaP
167 population using a Kaplan-Meyer's test.

168

169 *2.8. Liver RNA extraction and sequencing*

170 For each biological replicate, the RNAqueous®-4PCR Kit (Ambion, Austin USA) was used to
171 extract the total RNA from 15 mg of liver according to manufacturer instructions. RNA-seq
172 libraries were prepared using the TruSeq Stranded mRNA sample Prep kit (Illumina, San
173 Diego, USA) and sequenced on an Illumina GAIIx sequencer as 75 bp reads by Hybrigenics-

Helixio (Clermont-Ferrand, France). The methods used for sequencing analysis are described in the SI.

2.9. Liver and egg metabolomics

Liver and egg samples (20-50 mg) were extracted in methanol/water/dichloromethane (2/1.4/2 v/v/v) using the protocol described by Beckonert et al. (Beckonert et al., 2007). The methods used for metabolomics analysis are described in the SI.

3. Results

3.1. Parental exposure leads to metabolic disruption in F1 progeny

The main goal of this paper was to determine the transgenerational impacts of BaP but putative metabolic disorders were also studied in F1 females to assess phenotype transmission from the F0 generation to F2 progeny. No difference in hepatosomatic and adiposomatic indexes were found in F1-BaP females despite a marked increase of liver lipid contents (1.7 fold, p=0.003) (Fig. 1a-c). In addition to steatosis, the liver sections of F1-BaP females showed hepatocytes with fewer cell contacts and irregular shapes, leukocyte infiltrates, and swollen blood vessels typical of a progression from nonalcoholic fatty liver disease (NAFLD) to nonalcoholic steatohepatitis (NASH) (Fig. 1d-g). For carbohydrate metabolism, no difference in basal glycaemia was found in F1-BaP females despite a marked decrease of fasting plasma insulin concentrations (0.4 fold, p=0.008) (Fig. 1h, i). However, no decrease in liver and muscle carbohydrate content was observed (Fig. 1j, k). To study the molecular mechanism associated with metabolic disruption, the liver transcriptomic signature of F1-BaP females was compared to control frogs. Liver transcriptomes of F1-BaP females showed differential transcription of 130 genes with down-regulation in 70% of cases. (Table S1). Kyoto Encyclopedia of Genes and Genomes (KEGG) pathway enrichment analyses of the differentially transcribed genes indicated a link between BaP-parental exposure and “Steroid biosynthesis” (40.4-fold, p=1.12 E-11), “Biosynthesis of antibiotics” (6.6-fold, p=1.36 E-8), “Terpenoid backbone biosynthesis” (22.5-fold, p=5.22 E-5), “Metabolic

pathways" (2-fold, p=1.09 E-4), "Pyruvate metabolism" (9.5-fold, p=0.007), "PPAR signaling pathway" (6.5-fold, p=0.02). General ontology (GO) terms enrichment analyses of the differentially transcribed genes indicated a link between BaP-parental exposure and "Sterol biosynthetic process" (64.9-fold, p=8.29 E-4), "Isoprenoid biosynthetic process" (43.3-fold, p=0.0019), "Response to yeast" (27.8-fold, p=0.0048), "Iron ion binding" (4.8-fold, p=0.018) (Fig. S1). These enriched pathways indicate global metabolic impairment encompassing lipid, carbohydrate and protein metabolism. However, to compare metabolic impairment occurring in F1 and F2 females, we manually assigned each gene to general pathways known to be affected in NAFLD or NASH pathology (Fig. 1l). Many differentially transcribed genes were associated with lipid metabolism and highlighted a marked downregulation of genes involved in cholesterol metabolism (from 0.06 to 0.45-fold) including *3-hydroxy-3-methylglutaryl-CoA reductase* (*hmgcr*), *3-hydroxy-3-methylglutaryl-CoA synthase 1* (*hmgcs1*), *isopentenyl-diphosphate delta isomerase 1* (*idi1*), *methylsterol monooxygenase 1* (*msmo1*), *cytochrome b5 reductase 2* (*cyb5r2*), *acetyl-CoA acetyltransferase 2* (*acat2*), *mevalonate diphosphate decarboxylase* (*mvd*), *squalene epoxidase* (*sqle*), *lanosterol synthase* (*lss*), *7-dehydrocholesterol reductase* (*dhcr7*), *hydroxysteroid* (*17-beta*) *dehydrogenase 7* (*hsd17b7*), *sterol-C5-desaturase* (*sc5d*), *24-dehydrocholesterol reductase* (*dhcr24*), *cytochrome P450 51A1* (*cyp51a1*), *cytochrome P450 7A1* (*cyp7a1*) and *NAD(P) dependent steroid dehydrogenase-like* (*nsdhl*) (Fig. 1l). A large number of genes involved in fatty acid metabolism (*fatty acid amide hydrolase, faah.1; acyl-CoA synthetase 2.2, acss2.2; lysophosphatidylglycerol acyltransferase 1, lpgat1; lipase, hormone-sensitive, lipe*) and transport (*solute carrier family 27 member 4, slc27a4*) were downregulated. Only the gene encoding for solute carrier family 27 member 6 (*slc27a6*), involved in long chain fatty acid transport across membranes was upregulated (2.43-fold) (Fig. 1l). Analysis of genes involved in carbohydrate metabolism and insulin signaling pathways showed activation of *phosphoenolpyruvate carboxykinase 1* (*pck1*, 36.4-fold) and *insulin like growth factor binding protein 1* (*igfbp1*; 5.28-fold) genes (Fig. 1l). Among the genes involved in protein metabolism, there was a marked deregulation of the genes encoding HSP 70 and HSP 90 proteins (0.18

and 0.35-fold) suggesting endoplasmic reticulum stress (ER-stress). ER-stress has been associated with cell death and apoptosis (Faitova et al., 2006). We found that *DNA damage inducible transcript 4* (*ddit4*) and *protein tyrosine phosphatase 4A1* (*ptp4a1*) genes that are involved in the activation of cell death during stress (Chen et al., 2016; Halle et al., 2007) were upregulated (3.86 and 2.42-fold) (Fig. 1l). Analysis of genes associated with the immune system confirmed the histological data indicating an inflamed liver condition (Fig. 1d-g). Indeed, genes promoting inflammation (*signal transducer and activator of transcription 4, stat4; macrophage scavenger receptor 1, msr1; DEXD/H-box helicase 58, ddx58 and interleukin 18 binding protein –like, il18bp*) were upregulated (Fig. 1l). Thus, a histological phenotype highlighting decreased cell-cell contact was confirmed by the downregulation of genes involved in tight-junction integrity including *cadherin related family member 4* (*cdhr4,* 0.25-fold) and *F11 receptor* (*f11r*, 0.35-fold) genes (Fig. 1l).

3.2. F0-exposure to BaP leads to transgenerational impairment of F2 development and metabolism.

The F2 progeny from F0 frogs exposed to BaP had significantly delayed metamorphosis (p=2 E-16) (the 50% population metamorphosis level was reached 20 days later) compared to the control (Fig. 2a). In addition, F2 females from BaP exposed animals also showed delayed sexual maturity (p= 8 E-04), taking more than 80 days to reach 80% of mature *Xenopus* in the population compared to the controls (Fig. 2b). Analysis of metabolic disorders in sexually mature F2-BaP females showed increased hepatosomatic (1.2 fold, p=0.043) and adiposomatic (1.8 fold, p=0.026) indexes (Fig 2c, d). The liver sections of F2-BaP females had hepatocytes with fewer cell contacts and irregular shapes, leukocyte infiltrates, and swollen blood vessels (Fig. 2e-h). In carbohydrate metabolism, fasting glycaemia was increased in F2-BaP females compared to the controls without modification of fasting plasma insulin concentrations (Fig. 2i, j). To determine if the increase in fasting glycaemia in F2-BaP females was due to default in cell glucose assimilation, we performed glucose tolerance tests. Intraperitoneal injection of glucose led to a higher increase in the blood glucose level of

F2-BaP females compared to the controls. At 6-hours post-glucose injection, glycaemia of F2-BaP females was about 1.4 times that of controls (p=0.008) (Fig. 2k). This glucose intolerance was accompanied by a decrease in muscle glycogen stores (Fig. 2l). To determine if the observed-glucose intolerance and the subsequent decrease in carbohydrate contents in muscle was linked to insulin resistance, we monitored glycaemia after insulin injection. Interestingly, F2-BaP females did not display insulin resistance (Fig. 2m). However, by monitoring plasmatic insulin concentrations after glucose injection, we found a marked reduction in insulin secreting capacities of F2-BaP females (0.5 fold, p=0.005). Plasmatic insulin concentrations, measured 30 minutes after glucose injection, were 2.2-times lower in F2-BaP females than in the controls (Fig. 2n). At the histological level, a non-significant decrease (p=0.57) in insulin production by the pancreatic β-cells was observed between F2-BaP females comparatively to controls (Fig. S2). However, pancreatic sections revealed an increase in leukocyte infiltrates in F2-BaP females compared to the controls (Fig. 2o).

3.3. Liver transcriptomic signature of F2-BaP females confirmes metabolic impairments.

To study the molecular mechanisms associated with metabolic disruption, the liver transcriptomic signature of F2-BaP females was compared to controls. Liver transcriptomes of F2-BaP females showed differential transcription of 104 genes with upregulation in 54% of cases (Table S2). KEGG pathway enrichment analyses of the differentially transcribed genes indicated a link between BaP-F0 exposure and “Steroid biosynthesis” (29.9-fold, p=1.58 E-5) and “Biosynthesis of antibiotics” (5.3-fold, p=1.58 E-4). GO-terms enrichment analyses of the differentially transcribed genes indicated a link between BaP-F0 exposure and “Regulation of cell growth” (18.8-fold, p=0.01), “Sterol biosynthetic process” (48.1-fold, p=0.04), and “Establishment of protein localization to plasma membrane” (48.1-fold, p=0.04) (Fig. S3). We manually assigned each gene to general pathways known to be affected in NAFLD or NASH pathology (Fig. 3a). Many differentially transcribed genes were associated with lipid metabolism and there was a marked upregulation of genes involved in cholesterol metabolism including 3-*hydroxy-3-methylglutaryl-CoA reductase* (*hmgcr*, 2.58-fold);

hydroxysteroid (17-beta) dehydrogenase 7 (*hsd17b7*, 1.98-fold), *cytochrome P450 51A1* (*cyp51a1*, 3.35-fold), *farnesyl-diphosphate farnesyltransferase 1* (*fdft1*, 2.07-fold), *methylsterol monooxygenase 1* (*msmo1*, 4.98-fold) and *squalene epoxidase* (*sqle*, 14.34-fold) (Fig. 3a). In addition, two genes involved in fatty acid and triglyceride metabolism (*1-acylglycerol-3-phosphate O-acyltransferase 4,* agpat4) and transport (*solute carrier family 27 member 3*, *slca27a3*) were downregulated. Transcriptomic data also revealed upregulation of genes encoding the steatosis protective proteins regulcalcin (*rgn*, 2.38-fold), sulfotransferase 2B1 (*sult2b1*, 2.27-fold) and *lipase hormone-sensitive (lipe,* 9.33) (Fig. 3a). Analysis of genes involved in carbohydrate metabolism and insulin signaling pathways revealed increased activation of *insulin like growth factor binding protein 1* gene (*igfbp1*; 2.86-fold) (Fig. 3a). In addition, *nuclear receptor 4A1* gene (*nr4a1*) involved in gluconeogenesis activation was downregulated (0.25-fold) together with upregulation of *prolactin regulatory element binding* gene (*preb*, 1.96-fold) known to inhibit liver glucose production (Fig. 3a). Compared to F1-BaP females, transcriptomic data did not reveal ER-stress or cell death markers in F2-BaP females. All genes involved in cell death/proliferation appeared to be strongly under-transcribed (Fig. 3a). Analysis of genes associated with the immune system confirmed the histological data and suggested an inflammatory liver state (Fig. 2e-h). Genes promoting inflammation appeared upregulated including *C-reactive protein 4,* (*crp4*, 4.09-fold), *eosinophil peroxidase* (*epx*, 2.39-fold) and *mitogen-activated protein kinase 8* (*map3k8*, 2.70-fold) (Fig. 3a). Thus, a histological phenotype highlighting decreased cell-cell contact was confirmed by the marked downregulation of *cadherin 10* (*cdh10,* 0.26-fold) and *claudin 15.1* (*cldn15.1*, 0.33-fold) genes involved in tight-junction integrity (Fig. 3a).

3.4. Liver metabolomic signature of F2-BaP females indicates impairment of amino acids, lipids and carbohydrate metabolism.

To compare the metabolic profiles of the liver from F2-BaP and control females, partial least squares-discriminant analysis (PLS-DA) was performed using the ^{1}H NMR spectra of the aqueous liver extracts. A PLS-DA model was then fitted on the filtered and centered data. A

valid and robust model was adjusted (A=2; R^2=97.3%; Q^2=0.89). The score plot showed clear discrimination between control and F2-BaP samples on the first axis (Fig. S4a). We found 17 discriminant metabolites between F2-BaP and control females (Fig. 3b). The levels of branched amino acids (leucine, Isoleucine and valine), aromatic amino acids (phenylalanine and tyrosine), acidic amino acid (glutamate) as well as threonine, proline and alanine were decreased in F2-BaP females. In addition, creatine and glutathione contents were decreased by 23.3% (p=0.024) and 20.9% (p=0.014), respectively, in F2-BaP females. Glucose contents were decreased by 14.3% (p=0.034) and glycogen contents increased by 48.1% (p=0.017) in F2-BaP females compared to controls. Formate and acetate contents were increased by 97.3% (p=0.024) and 52.6% (p=0.024) in F2-BaP females. Choline, an important component of the cell membrane, was significantly reduced (-16.6%, p=0.024) in F2-BaP females.

For liver lipid extracts, a PLS-DA model was fitted on filtered and Pareto-scaled data. A valid and robust model was adjusted (A=3; R^2=0.906; Q^2=0.739). The score plot showed clear discrimination between control and F2-BaP samples on the first axis (Fig. S4b). Triglyceride contents were increased by 19.91% (p=0.014) in F2-BaP females suggesting steatosis development. This phenomenon was confirmed by the increase of CH_3 fatty acid (1.56%, p=0.04), CH_2 fatty acids (3.16%, p=0.018) and unsaturated fatty acid (3.63%, p=0.023) contents in F2-BaP liver. In contrast, total cholesterol and free cholesterol were, respectively, decreased by 12.9% (p=0.007) and 10.6% (p=0.007) in F2-BaP females compared to the controls (Fig. 3b).

3.5. Transgenerational metabolic disruption of F2-BaP Xenopus is associated with reproductive defects.

We evaluated the gonadosomatic index as a proxy for the female body reserve investment into gonadal development. F2-BaP females had a decreased gonadosomatic index compared to controls (0.8 fold, p=0.035) (Fig. 4a). To compare the metabolic profiles of the eggs from F2-BaP and control females, partial least squares-discriminant analysis (PLS-DA)

was performed based on the ^{1}H NMR spectra of the aqueous and lipids extracts. PLS-DA models were then fitted on filtered and centered data. Two valid and robust models were adjusted for aqueous (A=3; R^2=0.342; Q^2=0.699) and lipid extracts (A=3; R^2=0.984; Q^2=0.924). The score plots showed a clear discrimination between control and F2-BaP egg samples on the first axis (Fig. S5a, b). Analysis of discriminative metabolites in aqueous extracts revealed a decrease in glutamine, histidine and tryptophan amino acids together with creatine and glutathione contents in eggs from F2-BaP females (Fig. 4b). In addition, citrate and ATP/ADP/AMP contents were also decreased, respectively, by 8.8% (p=0.02) and 10.4% (p= 0.025) in eggs from F2-BaP females. Among the aqueous metabolites, only butyrate increased (11.7%, p=0.033) in F2-BaP eggs (Fig. 4b). Analysis of discriminative lipid metabolites in F2-BaP eggs revealed decreased total cholesterol (-7.7%, p=0.0016), cholesterol ester (-8.6%, p=0.0073), free cholesterol (-5.3%, p=0.0016) and CH_3 fatty acids (-0.7, p=0.017) contents and a slight increase in triglyceride, CH_2 fatty acids, and monounsaturated fatty acid contents. Phospholipid contents slightly decreased by 4.8% (p=0.0053) in eggs from F2-BaP females compared to controls (Fig. 4b).

To assess F2 reproductive success, we mated five F2 pairs from both the control and F2-BaP group. Only 60% (3) of the F2-BaP females laid eggs compared to 100% (5) of the controls following stimulation (Fig. 4c). In addition, whereas amplexus was successful for 100% of the controls, is was successful for only 40% (2) of F2-BaP frogs (Fig. 4d). F2 mating of control frogs produced an average of 270 hatched eggs per mating pair. In contrast, no viable larvae were obtained from the F2-BaP frogs (Fig. 4e).

4. Discussion

Experimental and epidemiological evidence from humans and other mammals has demonstrated a correlation between ED exposure and metabolic diseases (Casals-Casas and Desvergne, 2011). Studies using rodent models have highlighted the potential of ED to cause multigenerational and transgenerational metabolic effects (Lee and Blumberg, 2019). However, the potential involvement of ED in metabolic impairments as a possible cause of

amphibian population decline has been largely neglected. We studied controlled exposures of *X. tropicalis,* throughout their life cycle, to the ED BaP at environmentally relevant concentrations such as could be found in “safe” drinking water (Health Canada, 2016; WHO, 2003). These levels of BaP induced a metabolic syndrome in *X. tropicalis* featuring a pre-diabetic state (Regnault et al., 2018). In the present study, we highlighted that parental exposure to BaP, can cause multigenerational and transgenerational metabolic impairments in *Xenopus* and reproductive failure in the F2 generation.

F1-BaP females, only exposed at the gamete stage, displayed marked liver steatosis associated with liver inflammation, swollen blood vessels and tissue integrity loss typical of a progression between NAFLD to NASH (Takahashi and Fukusato, 2014) (Fig. 1c-g). Inflammatory phenotype was confirmed by the upregulation of genes promoting inflammation (*stat4; msr1; ddx58 and il18bp*) and tissue integrity loss by the marked deregulation of genes involved in a tight junction (*cdhr4,* and *f11r*) (Fig. 1l). This phenotype could be induced through aryl hydrocarbon receptor (Ah-R) activation, since this nuclear receptor is involved in NAFLD/NASH and liver inflammatory processes in mice (Moyer et al., 2016). The F1 generation was exposed at the gamete which constitute critical time windows to induce epigenetic alterations across multiple generations. Recent findings have provided evidence of Ah-R activation in mediating these effects (Viluksela and Pohjanvirta, 2019). Multigenerational action of Ah-R is confirmed by the marked inhibition of genes involved in cholesterol metabolism. Ah-R can modulate the expression of a number of genes involved in the cholesterol synthesis pathway in mammals among which *hmgcr*, *hsd17b7*, *cyp51a1*, *and sqle* were deregulated in F1-BaP females (Tanos et al., 2012) (Fig. 1l). Ah-R induced steatosis is also associated with suppression of fatty acid oxidation (Lee et al., 2010) and F1-BaP females displayed a markedly decreased transcription of the *lipe* gene encoding a critical enzyme involved in triglyceride degradation and fatty acid oxidation (Reid et al., 2008). Fatty liver disease is associated with endoplasmic reticulum stress (ER stress) and apoptosis (Bechmann et al., 2012; Naik et al., 2013). We showed that F1-BaP females had a marked deregulation of genes coding for proteins involved in adaptive unfolded protein

response (UPR) (*hsp70* and *hsp90*) (Vincenz et al., 2013) together with genes involved in the activation of cell death during stress (*ddit4* and *ptp4a1*) (Chen et al., 2016; Halle et al., 2007) (Fig. 1l). ER stress is a primary event of insulin resistance development (Otoda et al., 2013). No difference in carbohydrate contents in muscle was observed suggesting the absence of muscle insulin resistance (Fig. 1 j). However, despite no difference in basal glycaemia (Fig. 1 h), transcriptomic data in liver revealed activation of the *pck1* gene (Fig. 1l) which could be linked to hepatic insulin resistance or insulinopenia (Bechmann et al., 2012; Gomez-Valades et al., 2008). However, the marked activation of *igfbp1*, associated with insulinopenia (Brismar et al., 1994), and the marked decrease of fasting plasma insulin concentrations (Fig. 1i) suggests a pancreatic insulin secretory defect. Overall, our results demonstrate that the phenotype observed in F1-BaP females was similar to that of F0 animals exposed during their entire life to BaP (Regnault et al., 2018). This suggests that multigenerational transmission of metabolic impairments can occur in frogs.

As previously stated, the major goal of this paper was to investigate the transgenerational metabolic impacts of BaP and their potential consequence on fitness. F2-BaP frogs had significantly delayed metamorphosis (an increase of 20 d for 50% of the population to reach frog metamorphosis) (Fig. 2a) similar to the F0 and F1 generations (Regnault et al., 2018). This demonstrated the transgenerational activity of this ED. These types of disturbances could play a major role in the amphibian population decline as the delayed metamorphosis reduces adult recruitment and reduces the chances for successful reproduction (Smith, 1987). Our data clearly showed that delayed metamorphosis in females was accompanied by delayed sexual maturity, taking more than 80 days to reach 80% of mature *Xenopus* in the population compared to the controls (Fig. 2b). Delayed sexual maturity of females was accompanied by reduced developmental capabilities of their progeny which would probably decrease their chances of survival in case of pond drying (Gomez-Mestre et al., 2013). Metabolic disorders were studied in sexually mature females. Despite having different regulation of genes associated with carbohydrate and lipid metabolism than that observed in

F0 and F1 animals, the underlying mechanisms also seemed to be associated with insulin secretion defects. F2-BaP females had an increased hepatosomatic index associated with a 20% increase in liver triglycerides. Liver steatosis associated with triglycerides and fatty acid accumulation suggest the development of NAFLD (Fig. 2c, 3b). This phenotype was confirmed by the marked activation of the genes encoding for regulcalcin, sulfotransferase 2B1 and *lipase hormone sensitive* known to protect liver from steatosis (Musso et al., 2013; Reid et al., 2008; Yamaguchi and Murata, 2013) suggesting a fight against lipid accumulation. In F2-BaP females, liver inflammation, swollen blood vessels and loss of tissue integrity highlighted the progression from NAFLD to NASH(Takahashi and Fukusato, 2014). This phenotype was confirmed by transcriptomic data showing a 4-fold increase in the transcription level of *crp4, epx and map3k8* genes. Crp increase in the liver has been associated with NAFLD and diabetes in mammals (Foroughi et al., 2016). In addition, decreased cell-cell contacts was confirmed by the downregulation of *cadherin* and *claudin 15* genes involved in tight-junction integrity (Fig. 3a).

An increase in basal serum glucose levels was found between F2-BaP females with no change in insulin levels (Fig. 2i, j) which constitutes a marked difference between F1- and F2-BaP progeny. F2-BaP females also displayed a reduction in glucose tolerance accompanied by a decrease in muscle glycogen stores (Fig. 2k, l). This phenotype was not associated with insulin resistance (Fig. 2m) as suspected in F0-BaP females (Regnault et al., 2018) but to marked insulin secretory capacity defects (Fig. 2n) as suggested by data from F1-BaP females. Transcriptomic data from liver showing a marked upregulation of the *igfbp1* (Brismar et al., 1994) gene confirmed the observed insulinopenia but other transcriptomic and metabolomic markers suggested complex retroaction mechanisms associated with high glycaemia levels. Indeed, metabolomics and transcriptomic data from the liver revealed a decrease in free and total cholesterol levels together with an increase of genes encoding for cholesterol synthesis including the key regulator *hmgcr* (Fig 3a, b). These results confirmed that low hepatocyte cholesterol levels are key activators of cholesterol synthesis (Burg and Espenshade, 2011). Surprisingly after fasting, high plasma glucose levels were associated

453 with liver glucose depletion and increased liver glycogen content (Fig. 3b). Here we can
454 hypothesize that inappropriate neoglucogenesis activation or inhibition of glycogen
455 degradation during fasting may occur in F2-BaP females leading to a reconstruction or a
456 maintenance of glycogen stores. However, this would not explain the higher blood glucose
457 content. This phenotype has been described in mammals experiencing chronic diabetes
458 (Ferrannini et al., 1990). The observed downregulation of *nuclear receptor 4A1* gene (*nr4a1*)
459 (Fig. 3a) involved in gluconeogenesis activation (Pei et al., 2006) might only be associated to
460 retro-control of supra-normal glycogen stores (Wise et al., 1997). Activation of
461 neoglucogenesis in F2-BaP females was also confirmed by liver depletion of amino acids
462 (Fig. 3b) especially alanine which is the major amino acid precursor of glucose in liver and
463 threonine which also contributes to glucose production in liver (Kaloyianni and Freedland,
464 1990). The decrease observed in the other amino acid contents together with glutathione has
465 been described in mammal diabetic models and suggests liver dysfunction (Chen et al.,
466 2019b; Furfaro et al., 2012).
467 BaP induced multi- and transgenerational impairments in carbohydrate, lipid and protein
468 metabolism associated to defects in insulin secretory capacities (Regnault et al., 2018). In
469 female amphibians a large component of liver metabolism is directed to the constitution of fat
470 bodies associated with reproduction or overwintering survival (Fitzpatrick, 1976; Wright,
471 2003). Liver dysfunction is likely to impair these crucial processes. Data from F2-BaP
472 females revealed a marked increase in the adiposomatic index (Fig. 2d) suggesting that the
473 large part of cholesterol or triglyceride contents of the liver had been directed to the fat body.
474 This increase in fat bodies was accompanied by a decrease in the gonadosomatic index in
475 F2-BaP females (Fig. 4a). In sexually mature amphibians, coelomic fat bodies largely support
476 gonadal growth and maturation over somatic tissues and this is supported by an inverse
477 relationship between coelomic fat body size and gonad size (Wright, 2003). In a healthy,
478 sexually mature female amphibian with a normal ovarian cycle, lipids are preferentially
479 allocated to vitellogenesis over deposition into fat depots. Females with large fat bodies
480 therefore highlight a defect in oocyte maturation (Wright, 2003). To study the reproductive

capacity of F2-BaP animals compared to the controls, we used semi-natural mating. Despite reaching sexual maturity, F2-BaP females showed a decrease in reproductive investment since only three of five females laid eggs (Fig. 4c). We also observed mating behavior problems in the F2-BaP group since only two of five amplexi were successful compared to all five in the controls (Fig. 4d). F2-control mating produced eggs with variable, but substantial, hatch rates but F2-BaP females did not produce any F3 progeny and had a complete lack of reproductive success (Fig. 4e). Variable hatch rates occur in natural matings of *X. tropicalis* (Showell and Conlon, 2009). However, the same trend was previously observed in F1-BaP frogs but it was less severe because an F2 generation was produced (Regnault et al., 2018). These results suggest that a BaP-F0 exposure can lead to reproductive defects that become progressively worse in successive generations. Exposure of amphibians to a widely distributed ED, such as BaP, under natural conditions might lead to a population decline. In female frogs, a defect in oocyte maturation or metabolite composition may explain the absence of viable progeny. As noted before, large fat bodies suggest a defect in oocyte maturation (Wright, 2003). Metabolomics data demonstrated that the egg composition of F2-BaP females was very different from that of controls (Fig. S5a, b). Analysis of discriminative metabolites in the F2-BaP group showed a decrease of total cholesterol, cholesterol ester and free cholesterol contents (Fig. 4b) which are essential for oocyte maturation. Cholesterol depletion in amphibian oocytes has been linked to oocyte maturation defects and impaired fecundity (Buschiazzo et al., 2011; Buschiazzo et al., 2012; Buschiazzo et al., 2008). Interestingly the metabolite profile variations of F2-BaP eggs matched the principal variations found in the liver especially for lipid contents (Fig. 3b and 4b). It is possible that disruption of lipid metabolism in the liver may lead to inappropriate lipid storage in the fat bodies and ultimately lead to immature oocytes with high lipid levels but low cholesterol contents. In addition, reduced reproductive success might also have a male component. Zebrafish data has shown the capacity of dioxin, another Ah-R ligand, to decrease reproductive success of males transgenerationally (Baker et al., 2014).

5. Conclusion

We focused on finding links between BaP exposure and potential amphibian population decline. The widespread BaP can induce severe multi- and transgenerational metabolic disorders in amphibians at concentrations that are still considered safe for human consumption. Parental exposure to BaP can negatively affect the development and fecundity of their progeny over two generations and lead to reproductive failure in the F2 generation. Our findings serve as a starting point for additional work to elucidate the role of ED acting as metabolic disruptors or obesogens as contributing causes of amphibian population decline. Our results demonstrate the transgenerational effects of ED, which may apply to amphibians and also to mammals, including humans.

Data access

The RNA-seq sequence data reported in this paper have been deposited on NCBI Gene Expression Omnibus (GEO) databse, https://www.ncbi.nlm.nih.gov/geo/info/submission.html (accession nº GSE150911).

Acknowledgements

We thank Oliver Ross (XpertScientific) for the English review of the revised manuscript. This work was funded by Communauté d'Universités et Établissements Université Grenoble–Alpes Initiatives de Recherche Stratégiques– Initiatives d'Excellence Grant, by the Federative Structure Environnemental and Systems Biology (BEeSy) of the Grenoble-Alpes University, by the CNRS-INSU EC2CO program and by the French National Research Program for Environmental and occupational Health of ANSES (2018/1/096). Additional support came from the Université Grenoble Alpes (ANR-15-IDEX-02) SYMER programs. C.R. received funding from the French Ministry of Higher Education and Research. M.U. was funded by the Région Auvergne–Rhône-Alpes. This work benefitted from the French GDR "Aquatic Ecotoxicology" framework which aims at fostering stimulating scientific discussions and collaborations for more integrative approaches.

Author contributions.

MR and SR conceived and designed the experiments; MU, SV, MDGC, CR, SS, JBF, MTF, CC, MR and SR performed the experiments; MU, SV, MDGC, CR, MTF, CC, MR and SR analyzed the data. SR wrote the MS.

Competing interests

The authors declare no competing interests.

References

U.S. Environmental Protection Agency (USPEA), EDSP21 Dashboard - Endocrine Disruptor Screening Program for the 21st century. Available at https://actor.epa.gov/edsp21/

Baker, T.R., et al., 2014. Dioxin induction of transgenerational inheritance of disease in zebrafish. Molecular and cellular endocrinology 398, 36-41. doi:10.1016/j.mce.2014.08.011.

Bechmann, L.P., et al., 2012. The interaction of hepatic lipid and glucose metabolism in liver diseases. Journal of hepatology 56, 952-964. doi:10.1016/j.jhep.2011.08.025.

Beckonert, O., et al., 2007. Metabolic profiling, metabolomic and metabonomic procedures for NMR spectroscopy of urine, plasma, serum and tissue extracts. Nature protocols 2, 2692-2703. doi:10.1038/nprot.2007.376.

Brismar, K., et al., 1994. Effect of insulin on the hepatic production of insulin-like growth factor-binding protein-1 (IGFBP-1), IGFBP-3, and IGF-I in insulin-dependent diabetes. The Journal of clinical endocrinology and metabolism 79, 872-878. doi:10.1210/jcem.79.3.7521354.

Burg, J.S., Espenshade, P.J., 2011. Regulation of HMG-CoA reductase in mammals and yeast. Progress in lipid research 50, 403-410. doi:10.1016/j.plipres.2011.07.002.

Buschiazzo, J., et al., 2011. Nongenomic steroid- and ceramide-induced maturation in amphibian oocytes involves functional caveolae-like microdomains associated with a cytoskeletal environment. Biology of reproduction 85, 808-822. doi:10.1095/biolreprod.110.090365.

Buschiazzo, J., et al., 2012. Cholesterol depletion affects the biophysical state of oocyte membranes disturbing amphibian fertilization. Cryobiology 65, 359.

Buschiazzo, J., et al., 2008. Inhibition of Bufo arenarum oocyte maturation induced by cholesterol depletion by methyl-beta-cyclodextrin. Role of low-density caveolae-like membranes. Biochimica et biophysica acta 1778, 1398-1406. doi:10.1016/j.bbamem.2008.03.004.

.

575 Carey, C., et al., 1999. Amphibian declines: an immunological perspective. Developmental
576 and comparative immunology 23, 459-472. doi:10.1016/s0145-305x(99)00028-2.
577 Casals-Casas, C., Desvergne, B., 2011. Endocrine disruptors: from endocrine to metabolic
578 disruption. Annual review of physiology 73, 135-162. doi:10.1146/annurev-physiol-
579 012110-142200.
580 Chen, L., et al., 2019a. TiO2 nanoparticles and BPA are combined to impair the development
581 of offspring zebrafish after parental coexposure. Chemosphere 217, 732-741.
582 doi:10.1016/j.chemosphere.2018.11.052.
583 Chen, M., et al., 2019b. Changes in hepatic metabolic profile during the evolution of STZ-
584 induced diabetic rats via an (1)H NMR-based metabonomic investigation. Bioscience
585 reports 39. doi:10.1042/BSR20181379.
586 Chen, R., et al., 2016. DNA damage-inducible transcript 4 (DDIT4) mediates
587 methamphetamine-induced autophagy and apoptosis through mTOR signaling pathway
588 in cardiomyocytes. Toxicology and applied pharmacology 295, 1-11.
589 doi:10.1016/j.taap.2016.01.017.
590 Chevalier, N., Fenichel, P., 2015. Bisphenol A: Targeting metabolic tissues. Reviews in
591 endocrine & metabolic disorders 16, 299-309. doi:10.1007/s11154-016-9333-8.
592 Chevalier, N., Fenichel, P., 2016. [Endocrine disruptors: A missing link in the pandemy of
593 type 2 diabetes and obesity?]. Presse medicale 45, 88-97.
594 doi:10.1016/j.lpm.2015.08.008.
595 Coimbra, A.M., et al., 2015. Chronic effects of clofibric acid in zebrafish (Danio rerio): a
596 multigenerational study. Aquatic toxicology 160, 76-86.
597 doi:10.1016/j.aquatox.2015.01.013.
598 Crump, D., et al., 2002. Exposure to the herbicide acetochlor alters thyroid hormone-
599 dependent gene expression and metamorphosis in Xenopus Laevis. Environmental
600 health perspectives 110, 1199-1205. doi:10.1289/ehp.021101199.

DeCourten, B.M., et al., 2019. Direct and indirect parental exposure to endocrine disruptors and elevated temperature influences gene expression across generations in a euryhaline model fish. PeerJ 7, e6156. doi:10.7717/peerj.6156.

Duarte-Guterman, P., et al., 2014. Mechanisms of crosstalk between endocrine systems: regulation of sex steroid hormone synthesis and action by thyroid hormones. General and comparative endocrinology 203, 69-85. doi:10.1016/j.ygcen.2014.03.015.

Faitova, J., et al., 2006. Endoplasmic reticulum stress and apoptosis. Cellular & molecular biology letters 11, 488-505. doi:10.2478/s11658-006-0040-4.

Fedorenkova, A., et al., 2012. Ranking ecological risks of multiple chemical stressors on amphibians. Environmental toxicology and chemistry 31, 1416-1421. doi:10.1002/etc.1831.

Ferrannini, E., et al., 1990. Influence of long-term diabetes on liver glycogen metabolism in the rat. Metabolism: clinical and experimental 39, 1082-1088. doi:10.1016/0026-0495(90)90170-h.

Fitzpatrick, L.C., 1976. Life history patterns of storage and utilization of lipids for energy in amphibians. American zoologist 16, 725-732

Foroughi, M., et al., 2016. Relationship between non-alcoholic fatty liver disease and inflammation in patients with non-alcoholic fatty liver. Advanced biomedical research 5, 28. doi:10.4103/2277-9175.176368.

Furfaro, A.L., et al., 2012. Impaired synthesis contributes to diabetes-induced decrease in liver glutathione. International journal of molecular medicine 29, 899-905. doi:10.3892/ijmm.2012.915.

Gomez-Mestre, I., et al., 2013. Mechanisms and consequences of developmental acceleration in tadpoles responding to pond drying. PloS one 8, e84266. doi:10.1371/journal.pone.0084266.

Gomez-Valades, A.G., et al., 2008. Pck1 gene silencing in the liver improves glycemia control, insulin sensitivity, and dyslipidemia in db/db mice. Diabetes 57, 2199-2210. doi:10.2337/db07-1087.

629 Halle, M., et al., 2007. Protein tyrosine phosphatases: emerging regulators of apoptosis. Cell
630 Cycle 6, 2773-2781. doi:10.4161/cc.6.22.4926.
631 Hammond, S.A., et al., 2015. Influence of temperature on thyroid hormone signaling and
632 endocrine disruptor action in Rana (Lithobates) catesbeiana tadpoles. General and
633 comparative endocrinology 219, 6-15. doi:10.1016/j.ygcen.2014.12.001.
634 Hayes, T.B., et al., 2011. Demasculinization and feminization of male gonads by atrazine:
635 consistent effects across vertebrate classes. The Journal of steroid biochemistry and
636 molecular biology 127, 64-73. doi:10.1016/j.jsbmb.2011.03.015.
637 Hayes, T.B., et al., 2006. Pesticide mixtures, endocrine disruption, and amphibian declines:
638 are we underestimating the impact? Environmental health perspectives 114 Suppl 1, 40-
639 50.
640 Hayes, T.B., et al., 2002. Hermaphroditic, demasculinized frogs after exposure to the
641 herbicide atrazine at low ecologically relevant doses. Proceedings of the National
642 Academy of Sciences of the United States of America 99, 5476-5480.
643 doi:10.1073/pnas.082121499.
644 Hayes, T.B., et al., 2010a. The cause of global amphibian declines: a developmental
645 endocrinologist's perspective. Journal of Experimental Biology 213, 921-933.
646 doi:10.1242/jeb.040865.
647 Hayes, T.B., et al., 2010b. Atrazine induces complete feminization and chemical castration in
648 male African clawed frogs (Xenopus laevis). Proceedings of the National Academy of
649 Sciences of the United States of America 107, 4612-4617.
650 doi:10.1073/pnas.0909519107.
651 Health Canada, 2016. Guidelines for Canadian Drinking Water Quality: Guideline Technical
652 Document — Benzo[a]pyrene. Water and Air Quality Bureau, Healthy Environments and
653 Consumer Safety Branch, Health Canada, Ottawa, Ontario.
654 Hedayatirad, M., et al., 2020. Transgenerational disrupting impacts of atrazine in zebrafish:
655 Beneficial effects of dietary spirulina. Comparative biochemistry and physiology.
656 Toxicology & pharmacology : CBP 230, 108685. doi:10.1016/j.cbpc.2019.108685.

Helbing, C.C., 2012. The metamorphosis of amphibian toxicogenomics. Frontiers in genetics 3, 37. doi:10.3389/fgene.2012.00037.

IUCN, 2019. The IUCN Red List of Threatened Species. Version 2019-3.

Kaloyianni, M., Freedland, R.A., 1990. Contribution of several amino acids and lactate to gluconeogenesis in hepatocytes isolated from rats fed various diets. The Journal of nutrition 120, 116-122. doi:10.1093/jn/120.1.116.

Kiesecker, J.M., 2002. Synergism between trematode infection and pesticide exposure: a link to amphibian limb deformities in nature? Proceedings of the National Academy of Sciences of the United States of America 99, 9900-9904. doi:10.1073/pnas.152098899.

Langlois, V.S., et al., 2010. Low levels of the herbicide atrazine alter sex ratios and reduce metamorphic success in Rana pipiens tadpoles raised in outdoor mesocosms. Environmental health perspectives 118, 552-557. doi:10.1289/ehp.0901418.

Lee, J.H., et al., 2010. A novel role for the dioxin receptor in fatty acid metabolism and hepatic steatosis. Gastroenterology 139, 653-663. doi:10.1053/j.gastro.2010.03.033.

Lee, M.K., Blumberg, B., 2019. Transgenerational effects of obesogens. Basic & clinical pharmacology & toxicology 125 Suppl 3, 44-57. doi:10.1111/bcpt.13214.

Major, K.M., et al., 2020. Early life exposure to environmentally relevant levels of endocrine disruptors drive multigenerational and transgenerational epigenetic changes in a fish model. Frontiers in Marine Science 7. doi:10.3389/fmars.2020.00471.

Moyer, B.J., et al., 2016. Inhibition of the aryl hydrocarbon receptor prevents Western diet-induced obesity. Model for AHR activation by kynurenine via oxidized-LDL, TLR2/4, TGFbeta, and IDO1. Toxicology and applied pharmacology 300, 13-24. doi:10.1016/j.taap.2016.03.011.

Musso, G., et al., 2013. Cholesterol metabolism and the pathogenesis of non-alcoholic steatohepatitis. Progress in lipid research 52, 175-191. doi:10.1016/j.plipres.2012.11.002.

Naik, A., et al., 2013. Genomic aspects of NAFLD pathogenesis. Genomics 102, 84-95. doi:10.1016/j.ygeno.2013.03.007.

685 Olivares-Rubio, H.F., et al., 2015. Relationship between biomarkers and endocrine-disrupting
686 compounds in wild Girardnichthys viviparus from two lakes with different degrees of
687 pollution. Ecotoxicology 24, 664-685. doi:10.1007/s10646-014-1414-4.
688 Opitz, R., et al., 2005. Description and initial evaluation of a Xenopus metamorphosis assay
689 for detection of thyroid system-disrupting activities of environmental compounds.
690 Environmental toxicology and chemistry 24, 653-664.
691 Orton, F., Tyler, C.R., 2015. Do hormone-modulating chemicals impact on reproduction and
692 development of wild amphibians? Biological reviews of the Cambridge Philosophical
693 Society 90, 1100-1117. doi:10.1111/brv.12147.
694 Otoda, T., et al., 2013. Proteasome dysfunction mediates obesity-induced endoplasmic
695 reticulum stress and insulin resistance in the liver. Diabetes 62, 811-824.
696 doi:10.2337/db11-1652.
697 Pei, L., et al., 2006. NR4A orphan nuclear receptors are transcriptional regulators of hepatic
698 glucose metabolism. Nature medicine 12, 1048-1055. doi:10.1038/nm1471.
699 Perera, B.P.U., et al., 2020. The role of environmental exposures and the epigenome in
700 health and disease. Environmental and molecular mutagenesis 61, 176-192.
701 doi:10.1002/em.22311.
702 Petersen, G., et al., 2007. Study on enhancing the Endocrine Disrupter priority list with a
703 focus on low production volume chemicals (European Commission). Available from:
704 http://ec.europa.eu/environment/chemicals/endocrine/pdf/final_report_2007.pdf.
705 Regnault, C., et al., 2018. Unexpected metabolic disorders induced by endocrine disruptors
706 in Xenopus tropicalis provide new lead for understanding amphibian decline.
707 Proceedings of the National Academy of Sciences of the United States of America 115,
708 E4416-E4425. doi:10.1073/pnas.1721267115.
709 Regnault, C., et al., 2016. Metabolic and immune impairments induced by the endocrine
710 disruptors benzo[a]pyrene and triclosan in Xenopus tropicalis. Chemosphere 155, 519-
711 527. doi:10.1016/j.chemosphere.2016.04.047.

712 Regnault, C., et al., 2014. Impaired liver function in Xenopus tropicalis exposed to
713 benzo[a]pyrene: transcriptomic and metabolic evidence. BMC genomics 15, 666.
714 doi:10.1186/1471-2164-15-666.
715 Reid, B.N., et al., 2008. Hepatic overexpression of hormone-sensitive lipase and adipose
716 triglyceride lipase promotes fatty acid oxidation, stimulates direct release of free fatty
717 acids, and ameliorates steatosis. The Journal of biological chemistry 283, 13087-13099.
718 doi:10.1074/jbc.M800533200.
719 Robert, J., et al., 2018. Water Contaminants Associated With Unconventional Oil and Gas
720 Extraction Cause Immunotoxicity to Amphibian Tadpoles. Toxicological sciences : an
721 official journal of the Society of Toxicology 166, 39-50. doi:10.1093/toxsci/kfy179.
722 Robert, J., et al., 2019. Developmental exposure to chemicals associated with
723 unconventional oil and gas extraction alters immune homeostasis and viral immunity of
724 the amphibian Xenopus. The Science of the total environment 671, 644-654.
725 doi:10.1016/j.scitotenv.2019.03.395.
726 Safholm, M., et al., 2014. Risks of hormonally active pharmaceuticals to amphibians: a
727 growing concern regarding progestagens. Philosophical transactions of the Royal
728 Society of London. Series B, Biological sciences 369. doi:10.1098/rstb.2013.0577.
729 Showell, C., Conlon, F.L., 2009. Natural mating and tadpole husbandry in the western
730 clawed frog Xenopus tropicalis. Cold Spring Harbor protocols 2009, pdb prot5292.
731 doi:10.1101/pdb.prot5292.
732 Skinner, M.K., 2014. Endocrine disruptor induction of epigenetic transgenerational
733 inheritance of disease. Molecular and cellular endocrinology 398, 4-12.
734 doi:10.1016/j.mce.2014.07.019.
735 Smith, D., 1987. Adult recruitment in chorus frogs: effects of size and date at metamorphosis.
736 Ecology 68, 344-350.
737 Swain, P., Nayak, S.K., 2009. Role of maternally derived immunity in fish. Fish & shellfish
738 immunology 27, 89-99. doi:10.1016/j.fsi.2009.04.008.

739 Takahashi, Y., Fukusato, T., 2014. Histopathology of nonalcoholic fatty liver
740 disease/nonalcoholic steatohepatitis. World journal of gastroenterology 20, 15539-
741 15548. doi:10.3748/wjg.v20.i42.15539.
742 Tanos, R., et al., 2012. Aryl hydrocarbon receptor regulates the cholesterol biosynthetic
743 pathway in a dioxin response element-independent manner. Hepatology 55, 1994-2004.
744 doi:10.1002/hep.25571.
745 Trapido, M., Ingeborg, V., 1996. On polynuclear aromatic hydrocarbons contamination levels
746 in the ecosystem of Lake Peipsi in the 1970s-1980s. . Hydrobiologia 338 185-190.
747 Urbatzka, R., et al., 2007. Endocrine disrupters with (anti)estrogenic and (anti)androgenic
748 modes of action affecting reproductive biology of Xenopus laevis: I. Effects on sex
749 steroid levels and biomarker expression. Comparative biochemistry and physiology.
750 Toxicology & pharmacology : CBP 144, 310-318. doi:10.1016/j.cbpc.2006.10.008.
751 Usal, M., et al., 2019. Concomitant exposure to benzo[a]pyrene and triclosan at
752 environmentally relevant concentrations induces metabolic syndrome with
753 multigenerational consequences in Silurana (Xenopus) tropicalis. The Science of the
754 total environment 689, 149-159. doi:10.1016/j.scitotenv.2019.06.386.
755 Viluksela, M., Pohjanvirta, R., 2019. Multigenerational and Transgenerational Effects of
756 Dioxins. International journal of molecular sciences 20. doi:10.3390/ijms20122947.
757 Vincenz, L., et al., 2013. Endoplasmic reticulum stress and the unfolded protein response:
758 targeting the Achilles heel of multiple myeloma. Molecular cancer therapeutics 12, 831-
759 843. doi:10.1158/1535-7163.MCT-12-0782.
760 WHO, 2003. Polynuclear aromatic hydrocarbons in Drinking-water. Background document
761 for development of WHO., Guidelines for drinking-water quality, 2nd ed, Addendum to
762 Vol. 2. Health criteria and other supporting information. (Eds) World Health Organization,
763 Geneva.

764 WHO, 2012. State of the science of endocrine disrupting chemicals in: Bergman, A.,
765 Heindelerrold, J.J., Jobling, S., Kidd, K.A., Zoeller, T. (Eds.). World Health Organization.,
766 Geneva.
767 Wise, S., et al., 1997. Effects of hepatic glycogen content on hepatic insulin action in
768 humans: alteration in the relative contributions of glycogenolysis and gluconeogenesis to
769 endogenous glucose production. The Journal of clinical endocrinology and metabolism
770 82, 1828-1833. doi:10.1210/jcem.82.6.3971.
771 Wright, K., 2003. Cholesterol, corneal lipidosis, and xanthomatosis in amphibians. The
772 veterinary clinics of North America. Exotic animal practice 6, 155-167.
773 doi:10.1016/s1094-9194(02)00022-1.
774 Xie, X., et al., 2019. Underlying mechanisms of reproductive toxicity caused by
775 multigenerational exposure of 2, bromo-4, 6-dinitroaniline (BDNA) to Zebrafish (Danio
776 rerio) at environmental relevant levels. Aquatic toxicology 216, 105285.
777 doi:10.1016/j.aquatox.2019.105285.
778 Yamaguchi, M., Murata, T., 2013. Involvement of regucalcin in lipid metabolism and
779 diabetes. Metabolism: clinical and experimental 62, 1045-1051.
780 doi:10.1016/j.metabol.2013.01.023.

781
782
783

Fig. captions

Fig. 1. Multigenerational effects of BaP on F1 females. a. Hepatosomatic index of F1-control and F1-BaP females. ($n_{Control} = 6$, $n_{BaP} = 21$). **b.** Adiposomatic index of control and F1-BaP females. ($n_{Control} = 6$, $n_{BaP} = 21$). **c.** Hepatic lipid content of F1-control and F1-BaP females. The images reveal the lipid droplets (red staining, Oil Red O; Scale bars, 75 µm.). The histogram represents the proportion of stained area in the livers. ($n_{Control} = 6$, $n_{BaP} = 10$). **d.** Hematoxylin and erythrosin staining of liver sections from F1-control females (Scale bars, 120 µm). **e.** Hematoxylin and erythrosin staining of liver sections from F1-BaP females (Scale bars, 120 µm). The asterisks indicate leukocyte infiltrates and the arrow indicates a dilated blood vessel. **f.** Hematoxylin and erythrosin staining of liver sections from F1-control females (Scale bars, 60 µm). **g.** Hematoxylin and erythrosin staining of liver sections from F1-BaP females (Scale bars, 60 µm). The asterisk indicates leukocyte infiltrate. ($n_{Control} = 6$, $n_{BaP} = 10$). **h.** Fasting glycaemia of F1-control and F1-BaP females ($n_{Control} = 6$, $n_{BaP} = 21$). **i.** Fasting plasma insulin concentrations of F1-control and F1-BaP females ($n_{Control} = 4$, $n_{BaP} = 8$). **j.** Muscle glycogen content of F1-control and F1-BaP females ($n_{Control} = 6$, $n_{BaP} = 10$). **k.** Liver glycogen content of F1-control and F1-BaP females ($n_{Control} = 6$, $n_{BaP} = 10$). Statistical analyses used Wilcoxon's test.Statistical analyses used Wilcoxon's test. The asterisks indicate a significant difference from the control: $^{**}P < 0.01$. **l.** Circos plot representing the overlap between the liver transcriptome of F1-BaP females and metabolic pathways. The genes considered are those involved in metabolic disorders, immune system pathway and histopathological consequences. Dysregulated genes and pathways are indicated outside the circle. The color scale indicates transcription ratios (log2 fold change) relative to the F1-control female. ($n_{Control} = 5$, $n_{BaP} = 6$).

Fig. 2. Transgenerational developmental and metabolic effects of BaP on F2 females. **a.** Development curves of F2 individuals from hatching to metamorphosis. The distributions of F2 individual development times were compared between the F2-control population and

F2-BaP population using a Kaplan-Meyer test to evaluate global curve difference ($n_{Control}$ = 216, n_{BaP} = 134). The asterisks indicate a significant difference from the control: ***, $p < 0.001$.. **b.** Development curves of F2 juvenile females from hatching to sexual maturity. The distributions of F2 female development times were compared between F2-control populations and F2-BaP population separately, using a Kaplan-Meyer test to evaluate global curve difference ($n_{Control}$ = 87, n_{BaP} = 44). The asterisks indicate a significant difference from the control: ***, $p < 0.001$. **c.** Hepatosomatic index of F2-control and F2-BaP females. ($n_{Control}$ = 16, n_{BaP} = 16). **d.** Adiposomatic index of F2-control and F2-BaP females. ($n_{Control}$ = 16, n_{BaP} = 16). **e.** Hematoxylin and erythrosin staining of liver sections from F2-control females (Scale bars, 75 µm). **f.** Hematoxylin and erythrosin staining of liver sections from F2-BaP females (Scale bars, 75 µm). The asterisks indicate leukocyte infiltrates and the arrow indicates a dilated blood vessel. **g.** Hematoxylin and erythrosin staining of liver sections from F2-control females (Scale bars, 40 µm). **h.** Hematoxylin and erythrosin staining of liver sections from F2-BaP females (Scale bars, 40 µm). The asterisk indicates leukocyte infiltrate ($n_{Control}$ = 10, n_{BaP} = 10). **i.** Fasting glycaemia of F2-control and F2-BaP females ($n_{Control}$ = 36, n_{BaP} = 22). **j.** Fasting plasma insulin concentrations of F2-control and F2-BaP females ($n_{Control}$ = 10, n_{BaP} = 10). **k.** Glucose tolerance test ($n_{Control}$ = 21, n_{BaP} = 12). **l.** Muscle glycogen content of F2-control and F2-BaP females ($n_{Control}$ = 16, n_{BaP} = 13). **m.** Insulin resistance test ($n_{Control}$ = 10, n_{BaP} = 8). **n.** Plasma insulin concentrations 30 minutes after glucose injection ($n_{Control}$ = 6, n_{BaP} = 6). **o**. Percentage of F2 females with pancreatic inflammation 30 minutes after glucose injection ($n_{Control}$ = 6, n_{BaP} = 6). Images show insulin immunostaining of pancreas from F2-control and F2-BaP females. Asterisks indicate leukocyte infiltrates. Statistical analyses were performed using Wilcoxon's test (c-d, i-n) and a khi² test (o). The asterisks indicate a significant difference from the control: * $P < 0.05$, ** $P < 0.01$.

838 **Fig. 3. Liver transcriptomic and metabolomic signatures of F2-BaP females. a.** Circos
839 plot representing the overlap between liver transcriptome of F2-BaP females and metabolic
840 pathways. The genes considered are those involved in metabolic disorders, immune system
841 pathway and histopathological consequences. Dysregulated genes and pathways are
842 indicated outside the circle. The color scale indicates transcription ratios (log2 fold change)
843 relative to F2-control females ($n_{Control} = 5$, $n_{BaP} = 5$). **b**. Percent change in discriminant
844 metabolites between liver from F2-control and F2-BaP females ($n_{Control} = 10$, $n_{BaP} = 10$).
845 Statistical analyses were performed using Wilcoxon's test with multiple testing correction.
846 The asterisks indicate a significant difference from the control: * $P < 0.05$, ** $P < 0.01$, *** $P <$
847 0.001. *Un. Fatty acids*: unsaturated fatty acids.

848

849 **Fig. 4. F2-BaP reproductive capacities. a.** Gonadosomatic index of F2-control and F2-Bap
850 females ($n_{Control} = 16$, $n_{BaP} = 16$). **b**. Percent change in discriminant metabolites between
851 eggs from the control and F2-BaP females ($n_{Control} = 12$, $n_{BaP} = 12$). *MU. Fatty acids*: Mono-
852 unsaturated fatty acids. **c.** Percentage of females having laid eggs ($n_{Control} = 5$, $n_{BaP} = 5$). **d.**
853 Percentage of successful amplexus ($n_{Control} = 5$, $n_{BaP} = 5$). **e.** Number of hatched eggs per
854 mating pairs ($n_{Control} = 5$, $n_{BaP} = 5$).

855

856

857

858

859

860

861

862

Fig.1

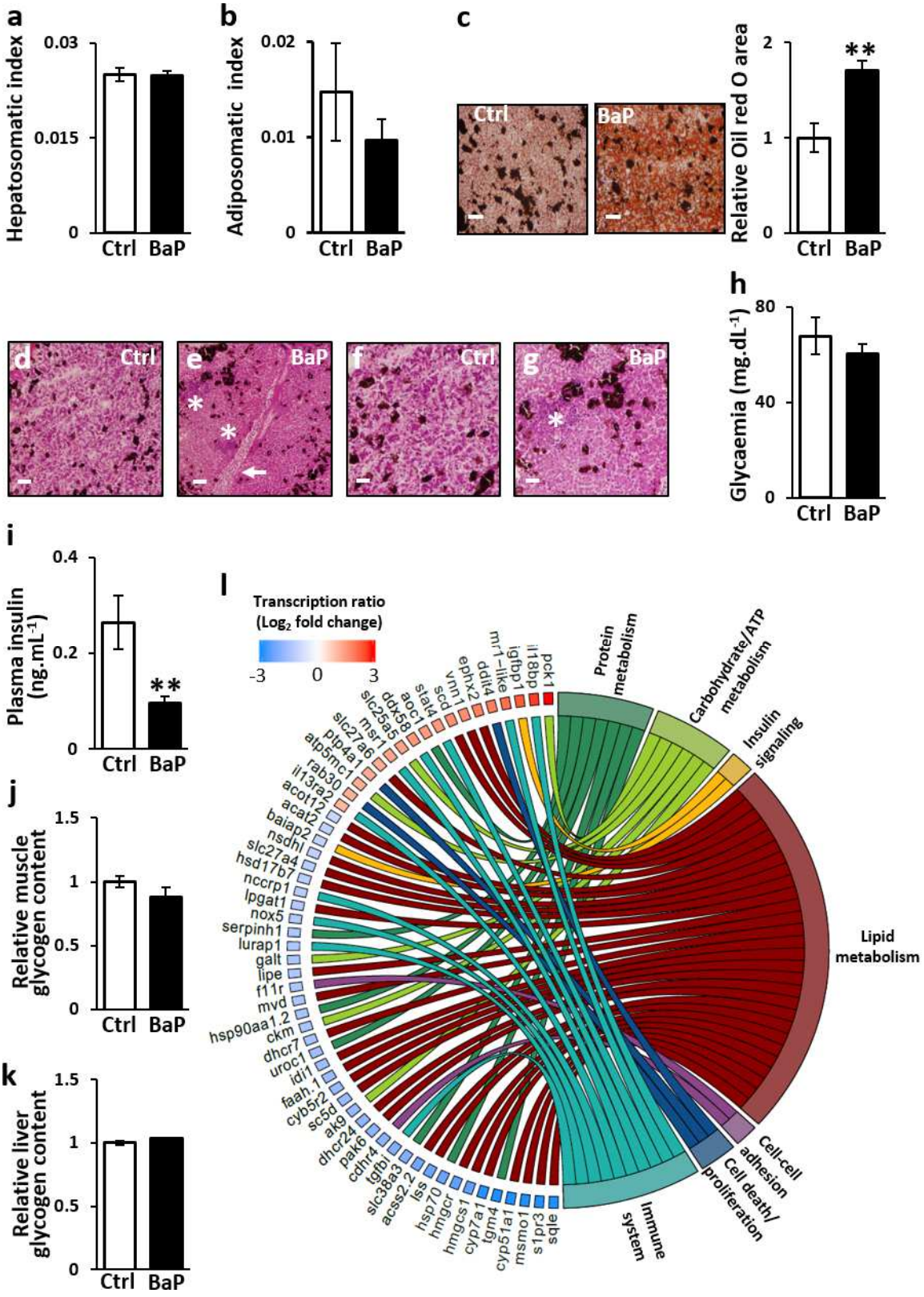
a
Hepatosomatic index
0.03
0.015
0
Ctrl
BaP
b
Adiposomatic index
0.02
0.01
0
Ctrl
BaP
c
Ctrl
BaP
Relative Oil red O area
2
1
0
**
Ctrl
BaP
d
Ctrl
e
BaP
f
Ctrl
g
BaP
h
Glycaemia (mg.dL-1)
80
40
0
Ctrl
BaP
i
Plasma insulin (ng.mL-1)
0.4
0.2
0
**
Ctrl
BaP
j
Relative muscle glycogen content
1.5
1
0.5
0
Ctrl
BaP
k
Relative liver glycogen content
1.5
1
0.5
0
Ctrl
BaP
l
Transcription ratio
(Log2 fold change)
-3
0
3
Protein metabolism
Carbohydrate/ATP metabolism
Insulin signaling
Lipid metabolism
Cell-cell adhesion
Cell death/ proliferation
Immune system
pck1
il18bp
igfbp1
mir1-like
ddit4
ephx2
vnn1
scd
slat4
aoc1
ddx58
slc25a5
msr1
slc27a6
ptp4a1
atp5mc1
rab30
il13ra2
acot12
acat2
baiap2
nsdhl
slc27a4
hsd17b7
nccrp1
lpgat1
nox5
serpinh1
lurap1
galt
lipe
f11r
mvd
hsp90aa1.2
ckm
dhcr7
uroc1
idi1
faah.1
cyb5r2
sc5d
ak9
dhcr24
pak6
cdhr4
tgfbi
slc38a3
acss2.2
lss
hsp70
hmgcr
hmgcs1
cyp7a1
tgm4
cyp51a1
msmo1
s1pr3
sqle

868 **Fig.2**

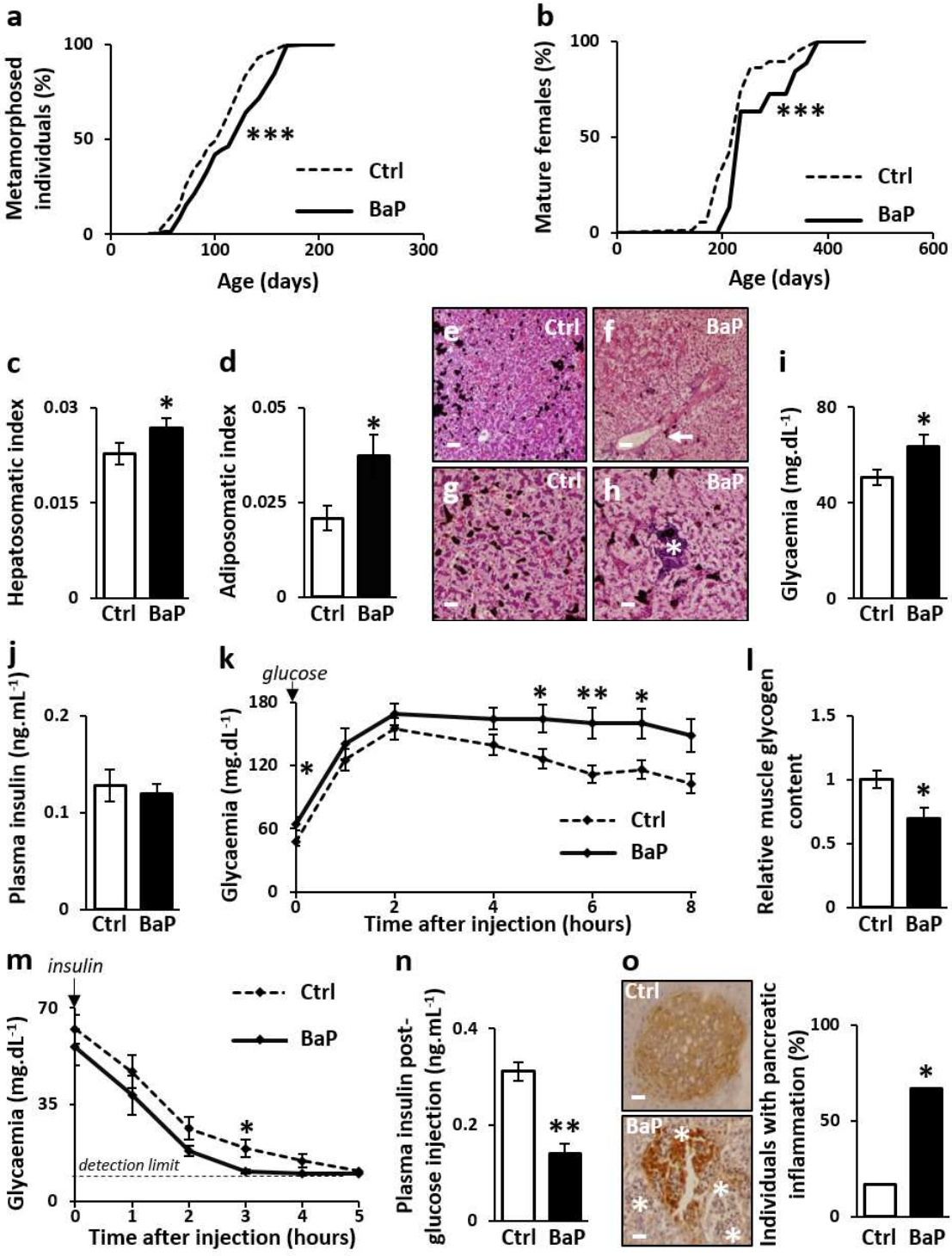

869

870

871 **Fig.3**

872

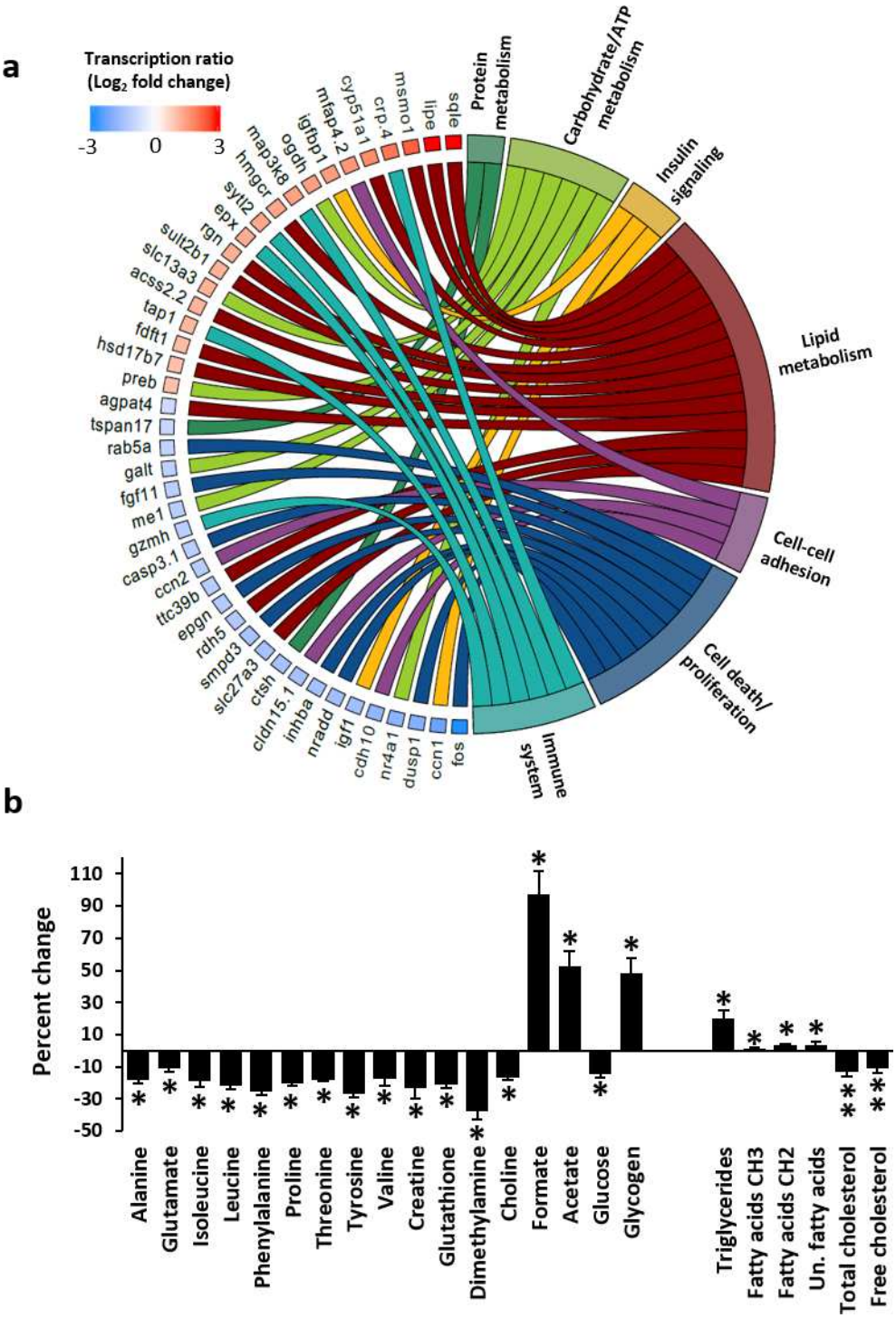

873

874

875

876 **Fig.4**

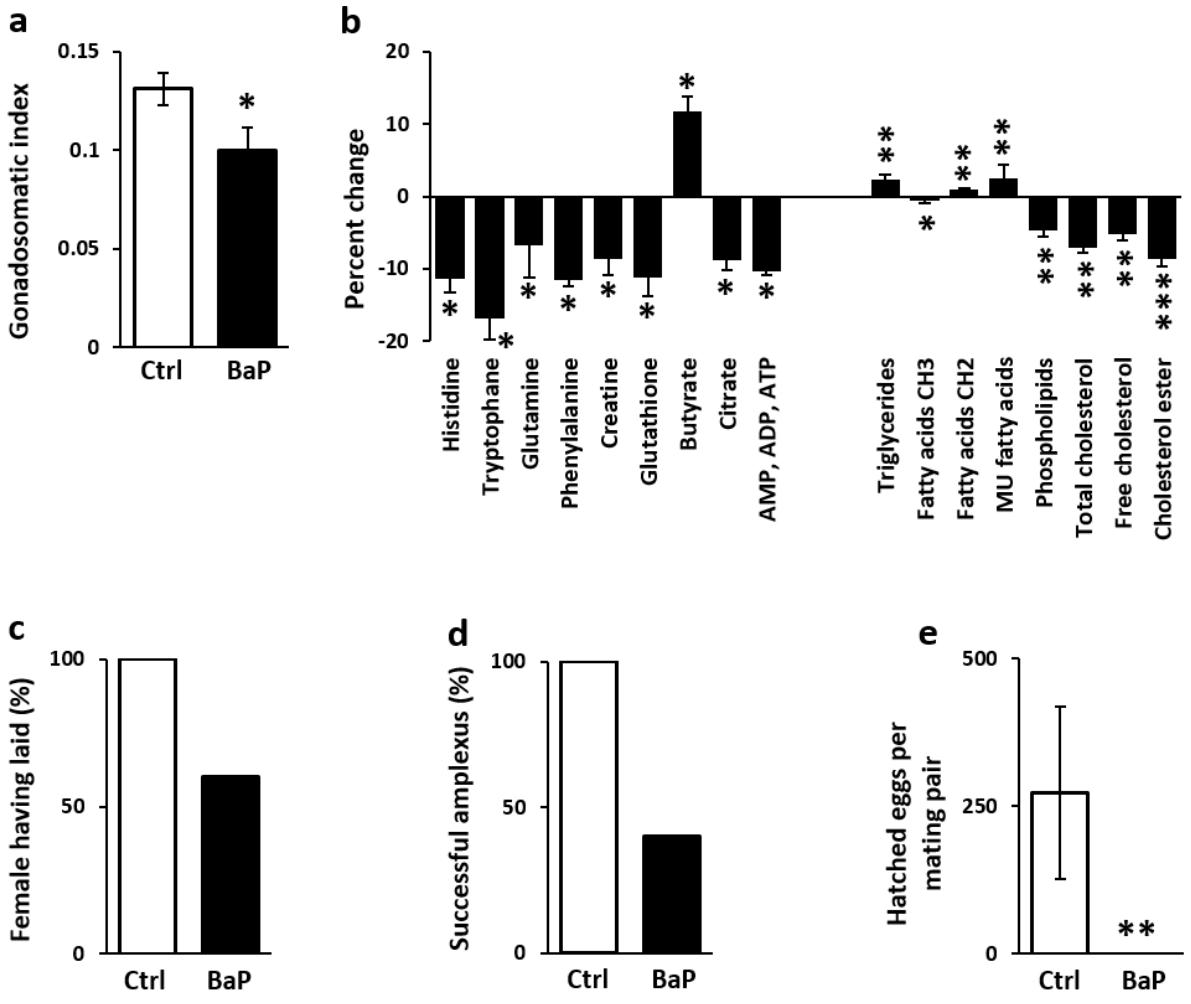

877

878

879

880

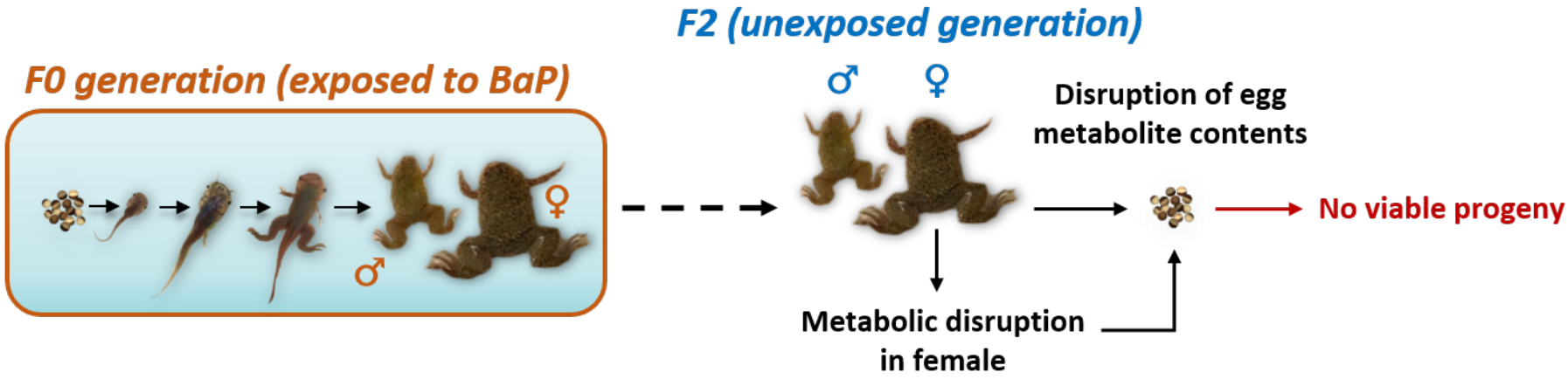
F0 generation (exposed to BaP)
♂
♀
F2 (unexposed generation)
♂
♀
Disruption of egg metabolite contents
No viable progeny
Metabolic disruption in female